

## Synthesis and Characterization of Vanadium Oxide ( $V_2O_5$ ) Thin Film Electrode for Electrochemical Capacitors: Effect of Annealing

M. S. Pawar<sup>1</sup>, M. A. Sutar<sup>2</sup>, K. I. Maddani<sup>3</sup> S. G. Kandalkar<sup>4</sup>

<sup>1</sup>Pimpri Chinchwad Polytechnic Pune, Maharashtra India,

<sup>2</sup>Y. B. Patil Polytechnic Pune Maharashtra India,

<sup>3</sup>S. D. M. college of engineering, Dharwad, Karnataka India,

<sup>4</sup>JSPM's Rajarshi Shahu College of Engineering, Tathawade, Pune, Maharashtra India

---

**Abstract:**  $V_2O_5$  thin film electrodes were synthesized by Successive Ionic Layer Adsorption and Reaction (SILAR) method on FTO substrate. Electrochemical performance of  $V_2O_5$  thin film electrode before and after annealing was studied. The structure, morphology and surface wettability were characterized by XRD, SEM and contact angle measurement, respectively. The optical band gap of  $V_2O_5$  thin film was increased from 2.06eV to 3eV after annealing. The electrochemical properties were examined by cyclic voltammetry and galvanostatic charge-discharge method. The specific capacitance of  $V_2O_5$  thin film electrode was decreased from 353 F/g to 301 F/g in 0.5M  $K_2SO_4$  electrolyte at scan rate of 10 mV/s. Specific energy and specific power decreased from 4.2 Wh/kg to 2.9 Wh/kg and 10.87 kW/kg to 8.38 kW/kg, respectively.

**Key Words:**  $V_2O_5$  electrode; specific capacitance; specific energy; specific power; annealing.

---

### I. Introduction

Conventional energy sources are likely to be depleted and on the way of finish. Looking closely at this fact, world have two alternatives 1) to find out production of renewable energy from nonconventional sources and 2) develop new smart storage devices to store the produced energy. This study emphasis on 2<sup>nd</sup> i.e. new smart storage devices to store the produced energy. Energy storage devices have fascinated great attention to fulfill increasing energy requirement and use energy efficiently.

Electrochemical capacitors (ECs) which are also known as supercapacitors are the energy storage devices having higher energy density than electrostatic capacitor, higher power densities than batteries, fast charge-discharge capability and long cycling life [1-7]. ECs store energy for electric vehicles (EVs) [8-9]. ECs, in which charge is accumulated on an electrode surface, are expected to serve as backup power supplies in EVs and power generators because of their high power densities [8-10]. Due to high operational parameters of the ECs, it has applications in many areas as energy storage devices, hybrid vehicles, engine starting devices for motor [11]. ECs and batteries are considered two of the most promising energy storage technologies for electric vehicles and renewable energy systems [12-15].

The electrode is the vital part of the ECs; therefore the electrode material is the main factor to determine the properties of ECs. The promising candidates as an electrode material include porous carbon materials, transition metal-oxides, conducting polymers and their derived composites [16-17].  $V_2O_5$  have been identified as electrode material for EC due to their low cost, abundance, and their potential pseudocapacitive characteristics [18-21]. Vanadium is resistant to corrosion because of formation of surface film oxide. At room temperature they are not affected by water, acids or air.  $V_2O_5$  has attracted much attention for EC applications because of its wide multifunctional properties [22].  $V_2O_5$  has highest oxidation state (saturated oxide), and therefore the most stable one, in the V-O system [23]. Vanadium oxide store energy like EDLC and also shows electrochemical faradic reactions between electrode material and ions [24].

Carbon materials [25-26], transition metal oxides [27-29] or hydroxides [30-31] and conducting polymers [32-33] are the extensively used electrode materials for ECs. Transition metal oxides and conductive polymers are frequently used as the Faradic redox pseudocapacitors [34]. Ruthenium oxide electrode shows high pseudocapacitance and good reversibility [35-37]. As ruthenium oxide is too expensive, is not cost effective for commercial applications [38]. Therefore, many efforts are made to search for alternative materials. Vanadium oxide material is of very much interest as it has many applications such as Gas sensors [39], electrochromic devices [40], electro-optic switches [41], CdTe solar cell with  $V_2O_5$  as a back contact buffer layer [42], Catalyst [43]  $V_2O_5$  has attracted much attention because of its layered structure, high capacity, etc. Previously  $V_2O_5$  was employed as the cathode material of Lithium-ion rechargeable battery [44-48].

In this work,  $V_2O_5$  thin film electrodes were prepared from vanadium chloride ( $VCl_3+H_2O$ ) precursor by simple non expensive SILAR method on FTO and effect of annealing was studied. Annealing of  $V_2O_5$  thin

film at 350<sup>0</sup>C for 4 hrs was done. The structural analysis was done by X-ray diffraction (XRD). The surface morphology of the film before annealing and after annealing was studied by scanning electron microscopy (SEM). The capacitive properties of the V<sub>2</sub>O<sub>5</sub> thin film electrodes were investigated by cyclic voltammetry and galvanostatic charge–discharge methods. The capacitive properties of the V<sub>2</sub>O<sub>5</sub> film electrode after annealing the film was also investigated by cyclic voltammetry and galvanostatic charge-discharge methods.

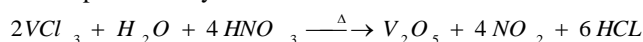
## II. Experimental

The V<sub>2</sub>O<sub>5</sub> thin films were deposited on fluorine doped tin oxide (FTO) substrate. Analytical reagent grade (AR) chemicals (VCl<sub>3</sub>: 99+ Merck Germany) were used for preparation of precursor solution. While optimizing preparative parameters like precursor solution concentration, dipping time and number of cycles were varied to procure good quality of V<sub>2</sub>O<sub>5</sub> thin films. The optimized parameters were as follows : 0.2 M VCl<sub>3</sub> in HPLC H<sub>2</sub>O , pH 1 was adjusted by HNO<sub>3</sub> drops, precursor solution temperature were maintained constant at 65<sup>0</sup> C. Vanadium oxide films were deposited from the cationic precursor of 0.2 M VCl<sub>3</sub> in H<sub>2</sub>O and addition of HNO<sub>3</sub> to make pH ~ 1 and the 0.1 % H<sub>2</sub>O<sub>2</sub> as anionic precursor. Double distilled water was alternately placed in between the beakers containing cationic and anionic precursor solutions. Cleaned FTO glass substrate was immersed into the cationic solution of VCl<sub>3</sub> for 40s, where vanadium ions were adsorbed on the substrate surface which was then rinsed with double distilled water for 15 s to remove loosely bounded vanadium ions from the substrate. The substrate was then immersed in anionic precursor (0.1% H<sub>2</sub>O<sub>2</sub>) solution for 20 s where the oxygen ion reacted with pre-adsorbed vanadium ions on the FTO glass substrate to form vanadium oxide film. The morphology and crystal structure of vanadium oxide thin films were investigated by scanning electron microscopy and X-ray diffraction techniques respectively. The electrochemical capacitive properties of V<sub>2</sub>O<sub>5</sub> film were investigated by cyclic voltammetry (CV) and galvanostatic charge-discharge methods in 0.5 M K<sub>2</sub>SO<sub>4</sub> aqueous solution. A three electrode cell was employed; V<sub>2</sub>O<sub>5</sub> thin films as working electrode and platinum electrode as a counter electrode. All electrochemical experiments were carried out at room temperature and all potential values given below refer to a saturated calomel electrode (SCE).

## III. Results And Discussion

### 3.1 Film Formation Mechanism

The deposition mechanism for V<sub>2</sub>O<sub>5</sub> film by SILAR is described as follows. The first deposition bath was made up of solution of VCl<sub>3</sub> in H<sub>2</sub>O some amount of HNO<sub>3</sub> was added and pH was adjusted to 1. After immersion of substrate in the first bath vanadium cations got adsorbed on the substrate surface. This was then rinsed in double distilled water to remove loosely bounded vanadium cations from the substrate. When this substrate was immersed in anionic solution (H<sub>2</sub>O + H<sub>2</sub>O<sub>2</sub>), oxygen anions reacted with pre-adsorbed vanadium cations and formation of vanadium oxide thin layer took place. Again substrate was rinsed in double distilled water to remove un-reacted oxygen anions. These four steps completed one deposition cycle of SILAR. After repeating such appropriate cycles, multilayer film formation of appropriate thickness took place on the substrate. Whole process may involve chemical reaction as follows



### 3.2 Structural and Morphological Analysis

Structural analysis of V<sub>2</sub>O<sub>5</sub> thin films was carried out by X-ray diffraction technique. Structural analysis of V<sub>2</sub>O<sub>5</sub> thin films was carried out on a Philips PW-1710 diffractometer by varying diffraction angle 2θ from 10<sup>0</sup> to 80<sup>0</sup>. Fig. 1 shows typical XRD pattern of V<sub>2</sub>O<sub>5</sub> thin film on FTO substrate. XRD pattern exhibited four peaks of V<sub>2</sub>O<sub>5</sub> as (2 3 3), (4 4 0), (0 4 6), (7 6 1). There was a good agreement with the JCPDS file (card no. 45-1074). One peak of FTO substrate was located at 2θ = 21.37<sup>0</sup> the sharpness of the peaks showed good crystallites. The V<sub>2</sub>O<sub>5</sub> film was polycrystalline. The small XRD peak intensities of vanadium oxide suggested the nanosize formation of grains.

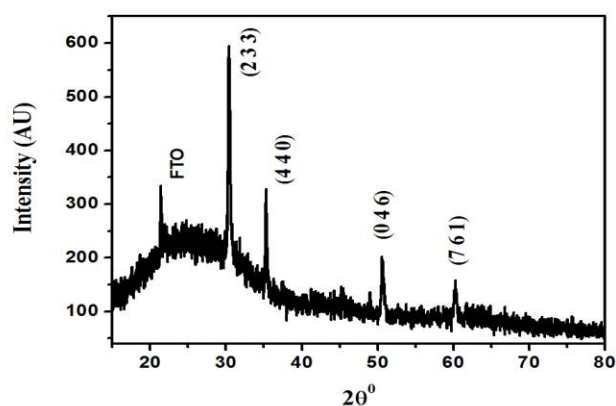


Fig. 1 X-ray diffraction pattern of as-deposited vanadium oxide thin film on FTO substrate.

The SEM image of the SILAR deposited  $V_2O_5$  thin film is shown in Figure 2(a). The substrate was well covered with small particles having different sizes. Some fine micro porous space between the particles was also observed. This type of morphology is favorable for ECs applications owing to its large surface area. Fig.2 (b) Shows SEM image of annealed  $V_2O_5$  thin film. Surface was covered with elongated particles which lead to increase in surface area. Some pin holes were also observed. In these cases the morphological changes might be taken place without improving the specific capacitance. After the annealing the morphology was attributed to increase in the porosity of the material because of reconstruction of particles [49].

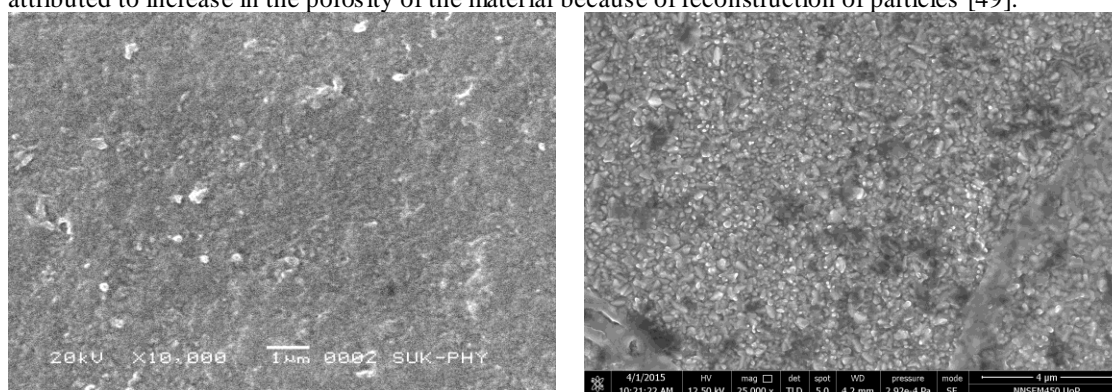


Fig. 2 The SEM image of the (a) as-deposited  $V_2O_5$  thin film (b) annealed  $V_2O_5$  thin film on FTO substrate.

### 3.3 Contact Angle Measurement

Fig. 3 shows water contact angle measurement of  $V_2O_5$  thin films onto FTO substrate. The observed water contact angle for as-deposited film was  $70^\circ$  and that of annealed film was  $73^\circ$ . It reveals the hydrophilic ( $\theta < 90^\circ$ ) behavior of  $V_2O_5$  thin film onto the FTO substrate. The hydrophilic nature of  $V_2O_5$  thin film electrode suggested that the films have potential application as an electrode material for ECs. Increase in water contact angle for  $V_2O_5$  thin film on FTO after annealing was attributed to the decrease in surface wettability and hence decrease in specific capacitance, it may be due to loss of hydroxide contents.

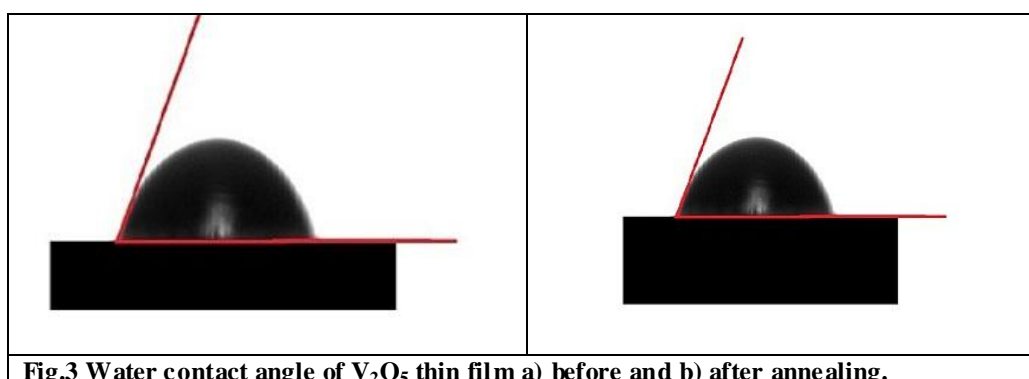


Fig.3 Water contact angle of  $V_2O_5$  thin film a) before and b) after annealing.

### 3.4 Optical Absorption and Band gap

The variation of absorbance ( $\alpha t$ ) with wavelength of  $V_2O_5$  films on FTO is shown in the Fig. 4. In case of as-deposited  $V_2O_5$  film on FTO substrate Fig. 4(a), absorbance decreased from 350nm to 475nm and after 475nm up-to 680nm rapid increase in absorbance was observed. After annealing Fig. 4(b), absorbance decreased sharply from 350nm to 490 nm and there after slow increase in absorbance was observed. The lowest absorbance of as-deposited  $V_2O_5$  film on FTO was at 475nm, but that of annealed  $V_2O_5$  film on FTO was at 500nm.

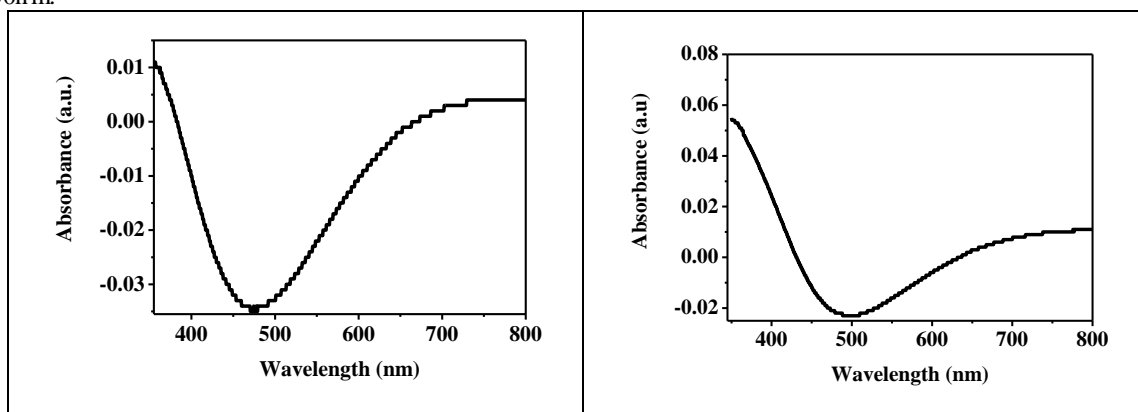


Fig. 4 Optical absorption characteristics of  $V_2O_5$  thin film on FTO substrate a) before annealing b) after annealing.

Fig. 5 shows the plots of  $(\alpha h\nu)^2$  versus  $h\nu$  for vanadium oxide film on FTO substrate. The calculated band gap energy for vanadium oxide film on FTO was 2.06 eV and that of annealed film was 3 eV. Band gap increased after annealing; indicates decrease in conductivity due to loss of hydroxide content. The band gap of  $V_2O_5$  is dependent on the experimental conditions and preparation methods [50-55].

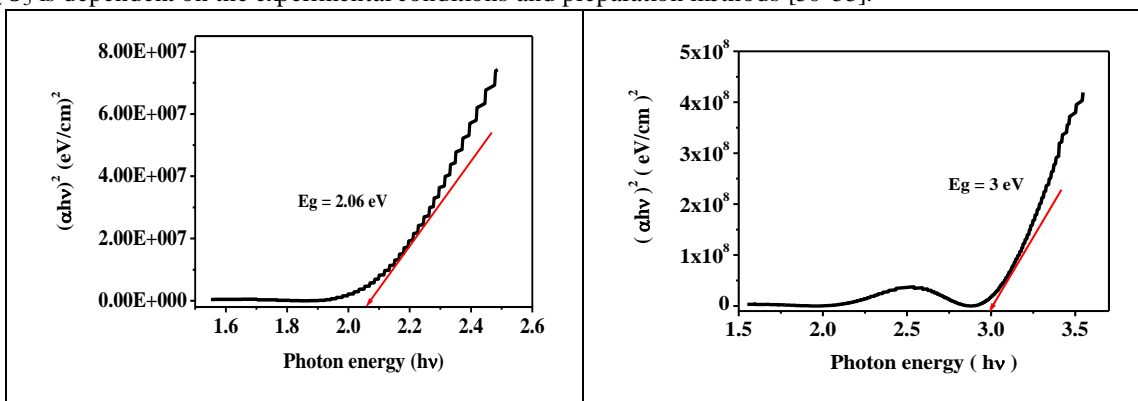


Fig. 5 The variation of  $(\alpha h\nu)^2$  vs.  $h\nu$  for  $V_2O_5$  thin film on FTO substrate a) as-deposited b) after annealing.

### 3.5. Supercapacitive Performance of $V_2O_5$ Thin Films

The cyclic voltammetry (CV) was considered to be an ideal tool to indicate the capacitive behavior of any material. Electrochemical performance of  $V_2O_5$  thin film electrode was tested using cyclic voltammetry (CV).  $V_2O_5$  thin film electrode with an area  $1 \text{ cm}^2$  were employed as working electrode. Saturated calomel electrode (SCE) served as the reference electrode while platinum electrode as counter electrode. Fig.6 shows the cyclic voltammetry (CV) curve of  $V_2O_5$  electrode at a scan rate of 10 mV/s within the potential from -0.2 to + 0.6 V vs. SCE in 0.5 M  $K_2SO_4$  electrolyte. From shape of CV it is confirmed that capacitance arises from redox transition and EDLC within the electrode/electrolyte and electrolyte/electrode interface, respectively. The capacitance was calculated from

$$C = \frac{I}{dV / dt}$$

Where 'I' was the average current,  $dV/dt$  was the scanning rate. The specific capacitance of the electrode was obtained by dividing the capacitance to weight (0.000112g) dipped in the electrolyte. The specific capacitance of the as-deposited  $V_2O_5$  electrode was found to be 353 F/g and that of annealed  $V_2O_5$  was

301 F/g in 0.5 M K<sub>2</sub>SO<sub>4</sub> electrolyte. Due to annealing the loss of hydroxide content causes decrease in conductivity of electrode and hence decrease in specific capacitance [56].

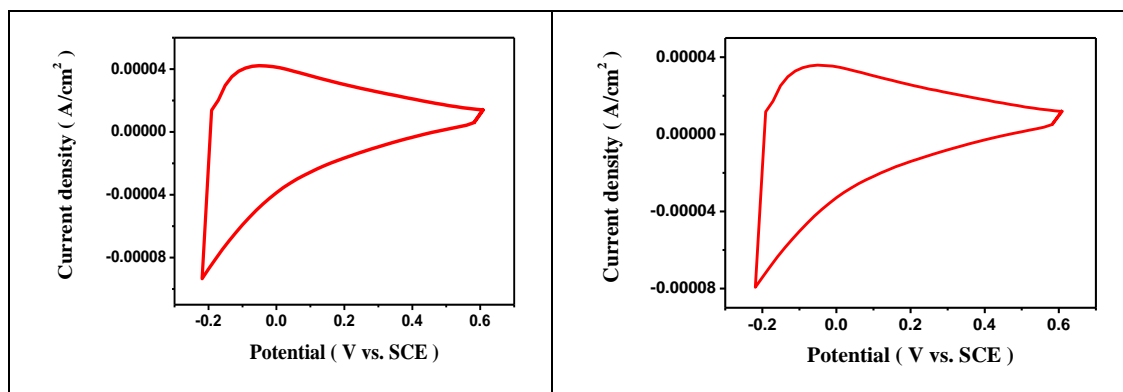


Fig. 6 CV curves of a) as-deposited b) annealed V<sub>2</sub>O<sub>5</sub> electrode in 0.5M of K<sub>2</sub>SO<sub>4</sub> electrolyte. The scanning rate was 10 mV/s.

### 3.6 Charge-Discharge Cycling Performance Measurements

The charge-discharge behavior of V<sub>2</sub>O<sub>5</sub> film electrode was studied by galvanometric charge-discharge method. Fig. 7 shows the charge-discharge behavior of electrode at the current density of 2 mA/cm<sup>2</sup>. The shape of discharge curve shows the capacitance characteristics of double layer capacitor. Linear variation of the time dependence of the potential indicates EDLC behavior. The electrical parameters, specific energy (E), and specific power (P) are calculated using the following equations

$$E = \frac{0.8 I_d T_d}{W} \dots\dots\dots (3)$$

$$P = \frac{0.8 I_d}{W} \dots\dots\dots (4)$$

Here, I<sub>d</sub> and T<sub>d</sub> are the discharge current and discharge time, respectively. The mass (W) of as-deposited V<sub>2</sub>O<sub>5</sub> thin film electrode was 0.0000112 gm/cm<sup>2</sup>. The values of specific energy (E), and specific power (P) obtained from Fig. 7a and 7b are 4.2 Wh/kg and 10.87 kW/kg respectively. After annealing, specific energy and specific power obtained are 2.9 Wh/kg and 8.38 kW/kg respectively.

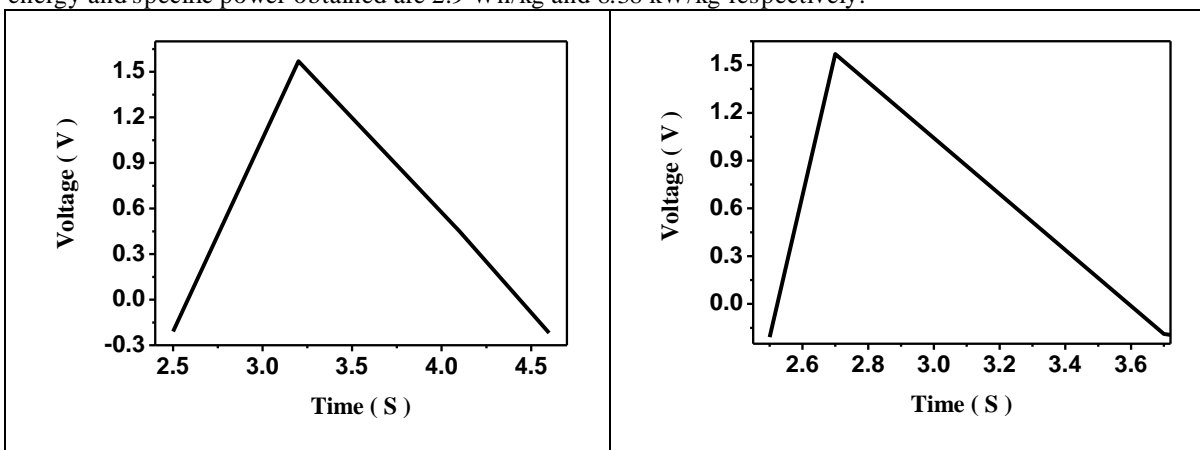


Fig. 7 Charge-discharge curve of a) as-deposited b) annealed V<sub>2</sub>O<sub>5</sub> electrode in 0.5 M K<sub>2</sub>SO<sub>4</sub> electrolyte. The charging current was 2 mA/cm<sup>2</sup>.

### IV. Conclusions

In summary, V<sub>2</sub>O<sub>5</sub> thin films prepared by SILAR method on FTO substrate. The XRD measurements confirmed that the V<sub>2</sub>O<sub>5</sub> were polycrystalline. The SEM analysis showed that the SILAR deposited V<sub>2</sub>O<sub>5</sub> thin film on FTO substrate was well covered with small particles having different sizes with some fine micro porous space between the particles and SEM image of annealed V<sub>2</sub>O<sub>5</sub> thin film showed surface was covered with

elongated particles with increase in surface area. The optical band gap of V<sub>2</sub>O<sub>5</sub> thin film was found to be 2.06 eV and of annealed film was found to be 3 eV.

The electrochemical study of V<sub>2</sub>O<sub>5</sub> electrode showed EDLC behavior. After annealing the specific capacitance of V<sub>2</sub>O<sub>5</sub> thin film electrode was decreased from 353 F/g to 301 F/g and specific energy and specific power decreased from 4.2 Wh/kg to 2.9 Wh/kg and 10.87 kW/kg to 8.38 kW/kg respectively in 0.5M K<sub>2</sub>SO<sub>4</sub> electrolyte at scan rate of 10 mV/s. The SILAR method is low cost and promisingly used for the fabrication of nanostructure material for ECs.

## References

- [1] K. Xie, B. Wei, Materials and structures for stretchable energy storage and conversion devices, *Adv. Mater.* 26(2014)3592–3617.
- [2] Khu Le Vann, ThuThuy Luong Thi, *Progress in Natural Science: Materials International* 24(2014)191–198.
- [3] M.R. Lukatskaya, O. Mashtalir, C.E. Ren, Y. Dall'Agnesse, P. Rozier, P.L. Taberna, M. Naguib, P. Simon, M.W. Barsoum, Y. Gogotsi, *J. Science* 341 (2013) 1502–1505.
- [4] X. Yang, C. Cheng, Y. Wang, L. Qiu, D. Li, *J. Science* 341(2013) 534–537.
- [5] D. Yu, K. Goh, H. Wang, L. Wei, W. Jiang, Q. Zhang, L. Dai, Y. Chen, *J. Nat. Nanotechnol.* 9(2014)555–562.
- [6] H.X. Ji, X. Zhao, Z.H. Qiao, J. Jung, Y.W. Zhu, Y.L. Lu, L.L. Zhang, A.H. MacDonald, R.S. Ruoff, *J. Nat. Commun.* 2(2014)18125–18131.
- [7] J. Yang, M.R. Jo, M. Kang, Y.S. Huh, H. Jung, Y.M. Kang *J. Carbon* 73(2014)106–113.
- [8] Wenhui Wang, Jiaolong Zhang, Yue Lin, Fei Ding, Zhenyu Chen, Changsong Dai, *Electrochimica Acta*, 170 (2015) 269–275.
- [9] Su F, Poh CK, Chen JS, Xu G, Wang D, Li Q, et al. *Energy Environ Sci* 2011;4(3):717–724.
- [10] Ding S, Zhu T, Chen JS, Wang Z, Yuan C, Lou XW. *J Mater Chem* 2011; 21(18):6602–6606.
- [11] Surovikin Yu. V. a, b *Procedia Engineering* 113 (2015) 511 – 518.
- [12] Z. Yu, *Energy Environ. Sci.* 8 (2015) 702–709.
- [13] P. Yang, W. Mai, *Nano Energy* 8 (2014) 274–280.
- [14] B. Dunn, *Science* 334 (2011) 928–935.
- [15] X. Lu, et al. *Energy Environ. Sci.* 7 (2014) 2160–2167.
- [16] R. Holze, Y.P. Wu, *J. Electrochim. Acta* 122 (2014) 93–107.
- [17] D.P. Dubal, R. Holze, *J. Pure Appl. Chem.* 86 (2014) 611–632.
- [18] G. Wang, X. Lu, Y. Ling, T. Zhai, H. Wang, Y. Tong, Y. Li, *ACS Nano* 6 (2012) 10296–10303.
- [19] S. Boukhalfa, K. Evanoff, G. Yushin, *Energy Environ. Sci.* 5 (2012) 6872–6879.
- [20] C.-H. Lai, C.-K. Lin, S.-W. Lee, H.-Y. Li, J.-K. Chang, M.-J. Deng, *J. Alloys Compd.* 536 (2012) 428–435.
- [21] J.-M. Li, K.-H. Chang, C.-C. Hu, *Electrochem. Commun.* 12 (2010) 1800–1807.
- [22] Z.J. Lao, K. Konstantinov, Y. Tournaire, S.H. Ng, G.X. Wang, H.K. Liu, *J. Power Sources* 162 (2006) 1451–1458.
- [23] R. Irani a, S.M. Rozati, S. Beke *Materials Chemistry and Physics* 139 (2013) 489–497.
- [24] Zhao D-D, Bao S-J, Zhou W-J, Li H-L. *Electrochem Commun.* 9 (2007) 869–877.
- [25] A.I. Najafabadi, T. Yamada, D.N. Futaba, M. Yudasaka, H. Takagi, H. Hatori, S. Iijima, K. Hata, *ACS Nano* 5 (2011) 811–818.
- [26] S. Vijayakumar, S. Nagamuthu, G. Muralidharan, *ACS Appl. Mater. Interfaces* 5 14 (2013) 2188–2196.
- [27] S.G. Kandalkar, D.S. Dhawale, Chang-Koo Kima, C.D. Lokhande, *Synthetic Metals* 160 (2010) 1299–1302.
- [28] S.G. Kandalkar, J.L. Gunjekar, C.D. Lokhande, Oh-Shim Joo, *Journal of Alloys and Compounds* 478 (2009) 594–598.
- [29] Q.T. Qua, Y. Shi a, L.L. Li a, W.L. Guo a, Y.P. Wua, H.P. Zhang b, S.Y. Guan b, R. Holze c, *Electrochemistry Communications* 11 (2009) 1325–1328.
- [30] Wang, Xiao-Feng, You Zheng, Ruan Dian-Bo, *Chinese J. Chem.*, 24 (2006) 1126.
- [31] C.C. Hu, J.C. Chen, K.H. Chang, *J. Power Sources* 221 (2013) 128.
- [32] Y.Q. Dou, Y. Zhai, H. Liu, Y. Xia, B. Tu, D. Zhao, X.X. Liu, *J. Power Sources* 196 (2011) 1608.
- [33] G.A. Snook, P. Kao, A.S. Best, *J. Power Sources* 196 (2011) 1.
- [34] B. Wang, J.S. Chen, Z.Y. Wang, S. Madhavi, X.W. (David) Lou, *Adv. Energy Mater.* 2 (2012) 1188–1192.
- [35] J.W. Liu, J. Essner, J. Li, *Chem. Mater.* 22 (2010) 5022–5030.
- [36] M.N. Patel, X.Q. Wang, B. Wilson, D.A. Ferrer, S. Dai, K.J. Stevenson, K.P. Johnston, *J. Mater. Chem.* 20 (2010) 390–398.
- [37] G.P. Zhang, L. Zhang, J.J. Zhang, *Chem. Soc. Rev.* 41 (2012) 797–828
- [38] Zeheng Yang , Feifei Xu , Weixin Zhang , Zhousheng Mei, Bo Pei, Xiao Zhu *Journal of Power Sources* 246. (2014) 24–31.
- [39] Chao Wang, Xiangdong Li, Feng Xia, Haibo Zhang, Jianzhong Xiao, *Sensors and Actuators B: Chemical*, 223, (2016), 658–663.
- [40] Zhongqiu Tong, Na Li, Haiming Lv, Yanlong Tian, Huiying Qu, Xiang Zhang, Jiupeng Zhao, Yao Li, *Solar Energy Materials and Solar Cells*, 146(2016)135–143.
- [41] Hongchen Wang, Xinjian Yi, Sihai Chen, Xiaochao Fu *Sensors and Actuators A: Physical*, 122(2005) 108–112.
- [42] Kai Shen, Ruilong Yang, Dezhao Wang, Mingjer Jeng, Sumit Chaudhary, Kaiming Ho, Deliang Wang, *Solar Energy Materials and Solar Cells*, 144 (2016) 500–508.
- [43] Siva Sankar Reddy Putluru, Leonhard Schill, Anita Godiksen, Raju Poreddy, Susanne Mossin, Anker Degn Jensen, Rasmus Fehmann , *Applied Catalysis B: Environmental*, 183(2016) 282–290.
- [44] Jing Pan, Ming Li, Yuanyuan Luo, Hao Wu, Li Zhong, Qiang Wang, Guanghai Li, *Materials Research Bulletin*, 74(2016) 90–95.
- [45] Huanqiao Song, Cuiping Zhang, Yaguang Liu, Chaofeng Liu, Xihui Nan, Guozhong Cao, *J. Power Sources*, 294(2015) 1–7.
- [46] Mohammad Ihsan, Qing Meng, Li Li, Dan Li, Hongqiang Wang, Kuok Hau Seng, Zhixin Chen, Shane J. Kennedy, Zaiping Guo, Hua-Kun Liu, *J. Electrochimica Acta*, 173(2015) 172–177.
- [47] Changlei Niu, Jingbo Li, Haibo Jin, Honglong Shi, Youqi Zhu, Wenzhong Wang, Maosheng Cao, *J. Electrochimica Acta*, 182(2015) 621–628.
- [48] Sinem Sel, Ozgur Duygulu, Umit Kadiroglu, Nesrin E. Machin, *J. Applied Surface Science*, 318(2014) 150–156.
- [49] J.P. Zheng, P.J. Cygan, T.R. Jow, *J. Electrochem. Soc.*, 142 (1995) 2699–2706.
- [50] A.A. Bahgat, F.A. Ibrahim, M.M. El-Desoky, *Thin Solid Films* 489 (2005) 68–75.
- [51] G.M. Wu, K.F. Du, C.S. Xia, X. Kun, J. Shen, B. Zhou, J. Wang, *Thin Solid Films* 485 (2005) 284–291.
- [52] L. Ottaviano, A. Pennisi, F. Simone, A.M. Salvi, *Opt. Mater.* 27 (2004) 307–314.
- [53] M. Benmoussa, A. Outzourhit, A. Bennouna, E.L. Ameziane, *Thin Solid Films* 405 (2002) 11–18

- [54] R.T. Rajendra Kumar, B. Karunakaran, S. Venkatachalam, D. Mangalaraj, Sa.K. Narayandass, R. Kesavamoothy, Mater. Lett. 57 (2003) 3820-3827.
- [55] Z.S. El Mandouh, M.S. Selim, Thin Solid Films 371 (2000) 259-266.
- [56] C.C. Hu, Y.H. Huang, K.H. Chang, J. Power Sources, 108 (2002) 117-124.